2012

Electrical transition of (3,3) carbon nanotube on patterned hydrogen terminated Si(001)-2 x 1 driven by electric field

Bikash C. Gupta
Virginia Commonwealth University

Shyamal Konar
Visva-Bharati University

Puru Jena
Virginia Commonwealth University, pjena@vcu.edu

Gupta, B. C., Konar, S., & Jena, P. Electrical transition of (3,3) carbon nanotube on patterned hydrogen terminated Si(001)-2 x 1 driven by electric field. Journal of Applied Physics, 111, 123717 (2012).

Electrical transition of (3,3) carbon nanotube on patterned hydrogen terminated Si(001)-2 × 1 driven by electric field

Bikash C. Gupta,[1,2,a)] Shyamal Konar,[2] and Puru Jena[1]
[1]*Department of Physics, Virginia Commonwealth University, Richmond, Virginia 23284, USA*
[2]*Department of Physics, Visva-Bharati, Santiniketan 731235, India*

(Received 3 April 2012; accepted 15 May 2012; published online 25 June 2012)

Structure, energetics, and electrical properties of (3,3) carbon nanotube (CNT) supported on patterned hydrogen terminated Si(001): 2 × 1 surface are studied using density functional theory. Our investigation reveals that an otherwise metallic (3,3) CNT when supported becomes semiconducting with a band gap of ≈0.5 eV due to its strong interaction with the surface. During adsorption, Si-C bonds form at the interface and charges transfer from Si surface to CNT. The Si-C bonds at the interface are partially covalent and partially ionic in nature. Under the application of an external electric field, the bandgap of the supported CNT reduces to zero, hence rendering the system metallic. © *2012 American Institute of Physics*. [http://dx.doi.org/10.1063/1.4729565]

I. INTRODUCTION

Carbon nanotubes (CNTs)[1] belong to an important class of nanomaterials for their novel electrical, mechanical, and optical properties. The outstanding properties of CNTs[2–8] make them suitable for potential technological applications. For instance, metallic CNTs may be used as one dimensional wiring material in circuit devices owing to their perfect one dimensional conducting behavior. These CNTs must be integrated with relevant substrate for large scale practical applications. Since silicon is easily available and Si(001) is one of the most stable surfaces, it is desirable to integrate CNTs on Si(001) surface. Naturally, the electronic properties of CNTs will be affected due to its interaction with the Si(001) surface. Hence, in order to have successful utilization of CNTs as wiring materials, a detailed understanding of the energetics, stability, electrical, and structural properties of CNTs supported on Si(001) surface is useful. Some investigations have been carried out in the past for understanding the interaction of CNTs[9–12] with bare Si(100):2 × 1 surface. Among them, Orellana *et al*. found that (6,6) CNT prefers to bind in between the dimer rows of bare Si(001): 2 × 1 and the metallic property of the CNT is enhanced. On the contrary, Berber and Oshiyama showed that a (5,5) CNT prefers to align along the perpendicular direction to dimer rows and the metallic character of the CNT disappears. Peng *et al*.[11] also found that a metallic (3,3) CNT favors to align itself in between Si dimer rows on bare Si(001):2 × 1 and loses its metallic character. Lopez *et al*.[12] considered adsorption of semiconducting CNTs on Si(001):2 × 1 and found that the semiconducting CNTs interact weakly with the surface. Further, a few adsorption studies of CNT on hydrogen terminated Si(001) surface[13–15] indicate that the CNTs have no preferential adsorption site; they are physisorbed and the properties of the CNTs are mostly preserved. Such observation is expected because hydrogen passivation makes the hydrogen terminated Si(001) surface chemically inert. However, one major problem is that it is not possible to have organized alignment of CNTs on bare Si(001) or on a fully hydrogenated Si(001) surface. One may overcome this difficulty by using an STM tip and creating preferential adsorption sites for CNT by removing selective hydrogen atoms from the fully hydrogen terminated Si(001) surface.[16,17] Depending on experimental conditions, a fully hydrogen terminated Si(001) surface may be reconstructed into any of 3 × 1, 1 × 1, and 2 × 1 phases.[18–25] As a fully hydrogen terminated Si(001): 2 × 1 is very stable and is easily obtained experimentally, it should be a good candidate for CNT integration. In fact, stabilization of single wall CNTs in hydrogen desorbed areas of the hydrogen terminated Si(001): 2 × 1 has been demonstrated[26–28] recently. Keeping in view of these experimental observations and possible applications of CNT as one dimensional conducting materials, we have studied the energetics, structure, and electrical properties of metallic (3,3) CNT supported on patterned Si(001): 2 × 1 surface. The metallic (3,3) CNT is chosen because it is one of the smaller diameter CNTs and it may be one of the synthesized CNTs with 4 Å diameter.[29] We further examine the effect of an external electric field on the electrical and structural properties of (3,3) CNT when it is supported on patterned hydrogen terminated Si(001): 2 × 1 surface. The significant observations in this study are: (1) the (3,3) CNT binds strongly with the patterned hydrogen terminated Si(001): 2 × 1 surface and in the process loses the metallic character. (2) The (3,3) CNT on the surface undergoes a metallic transition in the presence of an external electric field.

It is worth mentioning that there have been a number of studies on the tuning of electrical and structural properties of individual CNTs with strain, electric field, etc. However, not much attention has been paid yet on tuning the electrical properties of supported CNTs by external means. This is important from the technological point of view.

This paper is organized as follows. Section II describes the system, the method, and the relevant parameters. The results are discussed in Sec. III and finally we summarize our findings in Sec. IV.

a)Electronic address: bikashc.gupta@visva-bharati.ac.in.

II. APPROACH AND METHOD

First principle total energy calculations were carried out within the density functional theory at zero temperature using the VASP code.[30–33] The wave functions are expressed by plane waves with a cut off energy $|k+G|^2 \leq 500$ eV. The Brillouin zone (BZ) integrations are performed by using the Monkhorst-Pack scheme with $6 \times 6 \times 1$ k-point meshes for 4×2 primitive cells. Interaction between valence electrons and ion cores is represented by Vanderbilt type ultrasoft pseudo-potentials and results for fully relaxed structures are obtained using the PW91 generalized gradient approximation (GGA). The preconditioned conjugate gradient method is used for the wave function optimization and the conjugate gradient method for ionic relaxation. The convergence criteria for energy are taken to be 10^{-5} eV and the systems are relaxed until the forces are below 0.005 eV/Å.

The hydrogen terminated Si(001):2×1 is represented by a repeated slab geometry. Each slab consists of five atomic layers of Si. The top and the bottom layer Si atoms are passivated with hydrogen atoms. The top layer Si atoms dimerize and each surface Si atom is attached to a hydrogen atom (see Fig. 1). Thus, the hydrogen terminated Si(001): 2×1 surface consists of hydrogen terminated Si dimer rows. The consecutive slabs are separated by a vacuum space of ≈22 Å to avoid any interaction with its repeating image[34–37] when CNT is placed on the surface of the slab. The lateral inter-tube distance along X [110] direction is kept ≈11 Å to avoid inter-tube interaction. The Si atoms constituting top four layers of the slab along with the hydrogen atoms on the top are allowed to relax. The Si atoms of the bottom layer and the hydrogen atoms passivating the bottom-layer silicon atoms are kept fixed to simulate bulk like termination. The convergence with respect to the number of Si layers of the slab has already been examined earlier[34] and it was found that five Si layers are enough to realize the Si(001) surface. In order to have a periodicity match of the (3,3) CNT with the Si(001): 2×1 surface, the Si slab is squeezed along the Y [1$\bar{1}$0] direction by 3.25% and the consequent elastic expansion of the slab along X [110] and Z [001] directions is taken into consideration.[9]

The hydrogen terminated Si(001):2×1 surface is patterned by desorbing different groups of hydrogen atoms from the surface. We pattern the hydrogen terminated Si(001):2×1 surface in two reasonable ways: (1) All the hydrogen atoms attached to the right side Si dimers (see Fig. 1) within the 4×2 super-cell are removed and the resultant system is fully relaxed. The relaxed atomic structure of the patterned surface is shown in the Fig. 2. The pattern thus obtained for the hydrogen terminated Si(001) is termed as "Pattern-A." We note that the unpassivated Si dimers of the Si(001) surface with pattern-A are squeezed to 2.31 Å and buckled down with an angle of ≈19°. The Si(001) surface with pattern-A is modeled with 40 silicon atoms along with 20 hydrogen atoms within the 4×2 super-cell. (2) The hydrogen atoms occupying the region in between two consecutive Si dimer rows are removed within a 4×2 supercell. In other words, the hydrogen atoms attached to two consecutive Si dimer rows but facing each other are removed. The surface is then optimized to obtain the minimum energy structure. The relaxed structure of the surface in the form of a slab is shown in the Fig. 3. The surface pattern thus generated is termed as pattern-B. In this case, the alternative silicon dimers along the Y axis are buckled up and down by 6° and 12.6°, respectively. Again, this surface is realized with 40 Si atoms and 20 hydrogen atoms within the 4×2 super-cell.

For obtaining the relaxed atomic structure of (3,3) CNT on the Si(001) with pattern-A or pattern-B, the CNT is initially placed on top of the dangling bonds of the surface (hydrogen desorbed area of the surface) by aligning the tube axis parallel to the surface Si dimer rows extending along the Y [1$\bar{1}$0] direction (see Fig. 4). On both the patterned surfaces, the (3,3) CNT may be placed in two different orientations. First, the orientation of the CNT is such that one of the zigzag C-C chains of the CNT extending along the tube axis directly faces the surface. We may refer to this as *zigzag* orientation. Second, a row of parallel C-C bonds perpendicular to the CNT axis directly faces the surface, this orientation may be named as *parallel* orientation. To find the most stable geometry of the CNT on the surface, we calculate the binding energy (BE) of the CNT per unit length which is defined as

$$BE = \frac{E_{tot}[\mathrm{CNT} + \mathrm{Surf}] - E_{tot}[\mathrm{Surf}] - E_{tot}[\mathrm{CNT}]}{L}.$$

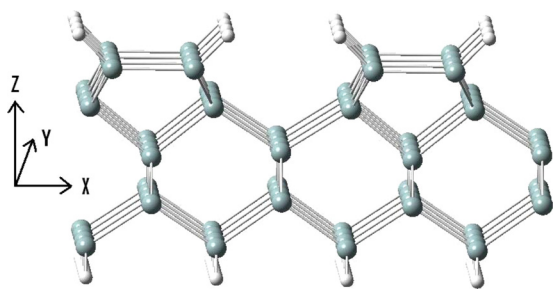

FIG. 1. Hydrogen terminated Si(001): 2×1 surface within the 4×4 cell. The bigger spheres correspond to the Si atoms while the smaller spheres represent the hydrogen atoms passivating the top and the bottom layer Si atoms. The surface has Si-dimer rows extending along the Y [1$\bar{1}$0] direction and the Si dimers are passivated with hydrogen atoms.

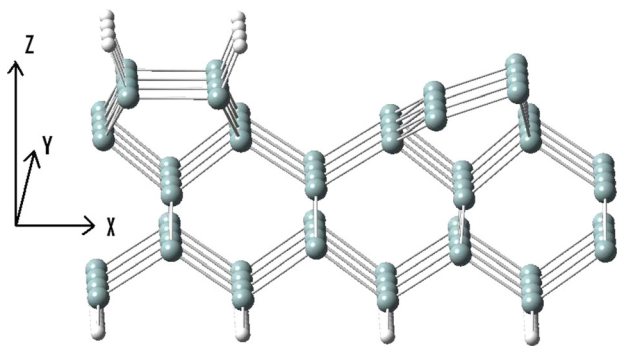

FIG. 2. Within the 4×4 cell, the relaxed atomic structure of the Si(001) with pattern-A is shown. The silicon and hydrogen atoms are represented by the bigger and smaller spheres, respectively. The unpassivated Si dimers are buckled.

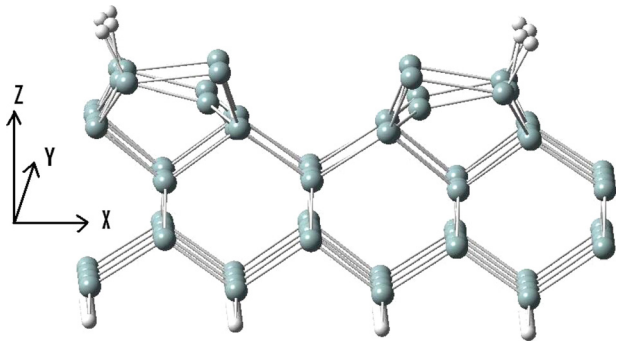

FIG. 3. Within the 4×4 cell, the relaxed atomic structure of the Si(001) with pattern-B is shown. The silicon and hydrogen atoms are represented by the larger and smaller spheres, respectively. The alternative silicon dimers are buckled up and down.

Here, E_{tot} [CNT + Surf] is the total energy of the integrated system (i.e., CNT(3,3) supported on Si(001) surface with pattern-A or pattern-B) within the 4×2 super-cell, E_{tot} [Surf] is the total energy of the Si(001) surface with pattern-A or pattern-B within the 4×2 super-cell, E_{tot} [CNT] is the total energy of the (3,3) CNT within the 4×2 super-cell, and L is the length of the CNT(3,3) within the 4×2 super-cell.

Analysis of most stable structures, band structures, density of states, work-function, and the effect of external electric field are discussed in Sec. III.

III. RESULTS AND DISCUSSIONS

A. (3,3) CNT on Si(001) with pattern-A

The energetically favorable relaxed atomic structure of (3,3) CNT on Si(001) with pattern-A is shown in the Fig. 5. The bucklings of Si dimers disappear and become flat due to CNT adsorption. The binding energy of the CNT per unit length is 0.75 eV/Å, which may differ from the practical value by a small amount due to forced commensuration of the CNT with the substrate in our calculation. The CNT resides 2.25 Å above the Si surface. It is clear from the figure that the relaxed structure prefers the *parallel* orientation. Two of three C-C bonds of the CNT which were initially located at the interface and oriented parallel to surface Si dimers break in order to form C-Si bonds. In the process of CNT adsorption, four C-Si bonds form at the cost of two C-C bonds of CNT and a net energy of 5.6 eV is gained within the 4×2 supercell. The C-C bond lengths of the CNT vary between 1.41 Å and 1.52 Å with an average length of

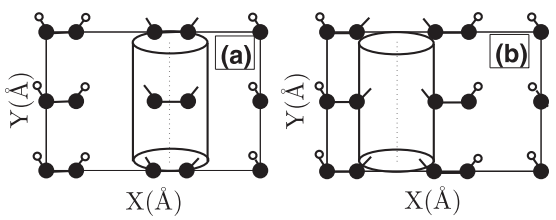

FIG. 4. In this schematic diagram, the initial positions of (3,3) CNT on the Si(001) are shown. The top layer Si and hydrogen atoms are represented by open (small) and filled circles (large), respectively. Panel (a) corresponds to Si(001) having pattern-A and the panel (b) corresponds to the Si(001) having pattern-B.

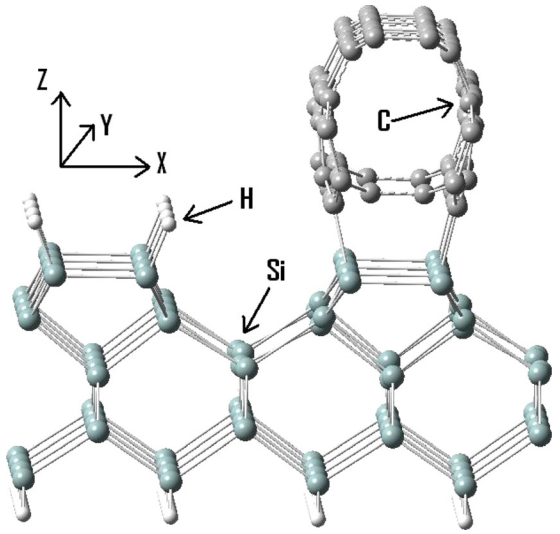

FIG. 5. The most favorable atomic structure of the CNT(3,3) placed on the hydrogen terminated Si(001) surface having pattern-A.

1.445 Å. The C-Si bond lengths are ≈1.90 Å. These imply that the CNT binds strongly with the Si(001) having pattern-A. In spite of strong interaction of the CNT with the surface, the hollowness of the CNT is retained with some deformations. A quantitative idea of deformation of the (3,3) CNT supported on a surface may be obtained by using a quantity called deformation ratio (ΔR) given by

$$\Delta R = \frac{(R_{max} - R_{min})}{R},$$

where R_{max} and R_{min} are the maximum and minimum radiuses of the (3,3) CNT after complete optimization of the CNT on the surface and R is the average radius of the relaxed (3,3) CNT.

According to the above definition, the deformation of the (3,3) CNT on the Si(001) with pattern-A is 18% which is an indication of strong binding of the CNT with the surface. However, this deformation is less compared to 26% deformation of (3,3) CNT on bare Si(001): 2×1 surface. This is reasonable because in contrast to bare Si(001): 2×1 surface, the surrounding of the CNT on the Si(001) with pattern-A is chemically inert due to hydrogen passivation.

An isolated (3,3) CNT is known to possess one dimensional metallic behavior. To find out if the CNT retains its metallic character on the Si(001) surface with pattern-A, we have plotted the band structure and density of states of the (3,3) CNT supported on the surface (see Fig. 6). From both the band structure and the density of states in Fig. 6, we find that the (3,3) CNT loses its metallic character and behaves like a semiconductor with a gap of 0.49 eV. Though the band gap around the fermi level turns out to be ≈0.49 eV in our density functional calculations, in practice, it must be larger than 0.49 eV. But the point to note is that (3,3) CNT undergoes a semiconducting transition due to its coupling with the Si(001) surface having pattern-A. To understand the coupling between CNT and the silicon surface further, we have plotted the partial charge density corresponding to the highest occupied band in Fig. 7. This shows that electronic charges

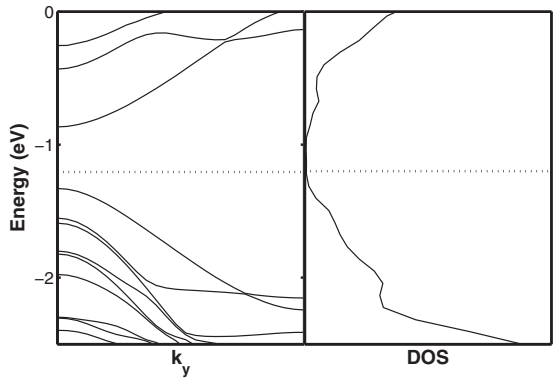

FIG. 6. The band structure and density of states of CNT(3,3) integrated on Si(001) with pattern-A. The dashed line indicates the fermi energy level.

from both carbon and silicon atoms are responsible in the formation of the highest occupied band and result from hybridization of carbon π states with silicon dangling bond states. Hence, π electrons which were responsible for conduction in an isolated (3,3) CNT become localized, opening a gap around the fermi level, thus turning it semiconducting.

To identify the nature of C-Si bonds, we have also carried out charge redistribution analysis by calculating the total charge density difference $\Delta\rho$ which is defined as

$$\Delta\rho = \rho[CNT + Si] - \rho[Si] - \rho[CNT],$$

where ($\rho[CNT]$) is the total charge density of isolated CNT, $\rho[Si]$ is the total charge density of the Si(001) surface on which CNT is integrated, and $\rho[CNT + Si]$ corresponds to the total charge density of the integrated system of CNT and Si(001) surface. Here, $\Delta\rho$ along a C-Si bond is plotted and shown in Fig. 8. It clearly indicates that charge transfer from Si to C has taken place along with some accumulation of charge in the middle of Si-C bond. Therefore, we may conclude that the Si-C bonds have a combination of ionic and covalent characters. A Bader charge analysis[38,39] confirms

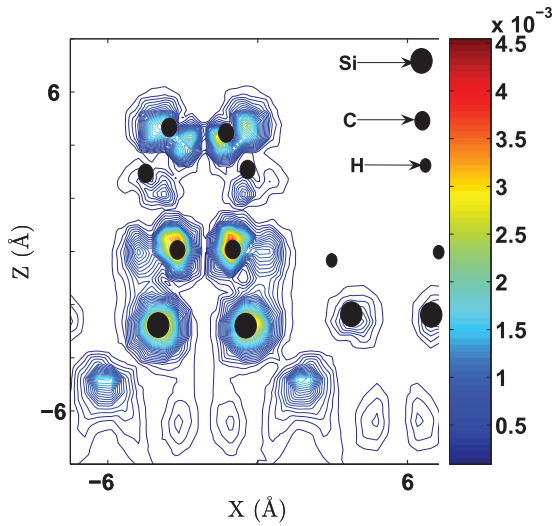

FIG. 7. Partial charge density plot for the highest occupied band of CNT(3,3) integrated on Si(001) having pattern-A. Note that electronic charges from both carbon and silicon are responsible in the formation of the highest occupied band.

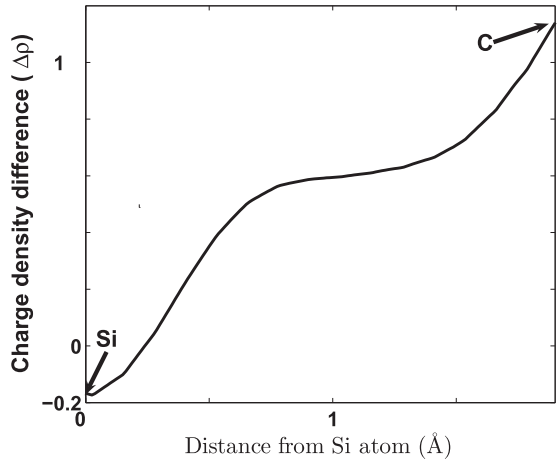

FIG. 8. Charge density difference, $\Delta\rho$, is plotted along Si-C bond of the most stable structure of CNT(3,3) integrated on the Si(001) having pattern-A.

that 2.27 e is transferred from Si surface to CNT within the 4×2 supercell. In general, charges are transferred from lower to a higher work-function material. To verify if direction of charge transfer in our system obeys this general trend, we have calculated the work-function of isolated CNT and the Si(001) having pattern-A separately. The work-function is calculated by taking the difference between the vacuum energy level (Φ_{av}) and the fermi energy level (E_F) and is defined as

$$WF = \Phi_{av} - E_F.$$

The vacuum level energy (Φ_{av}) is estimated by plotting the average electrostatic potential (averaged over the XY-plane) as a function of distance from the surface of the system. Figure 9 shows the average potential plots for (a) (3,3) CNT and (b) Si(001) having pattern-A. The vacuum levels as well as the fermi levels are shown in the figure. The work-function for the (3,3) CNT turns out to be 4.35 eV and that for the Si(001) having pattern-A is 4.50 eV. Thus, in contrary to the general trend, electronic charge transfers from the higher work-function material (Si(001) having pattern A) to a lower work-function material ((3,3) CNT). The direction of charge transfer may also depend on the hybridization between the adsorbate and substrate and the relaxation of the

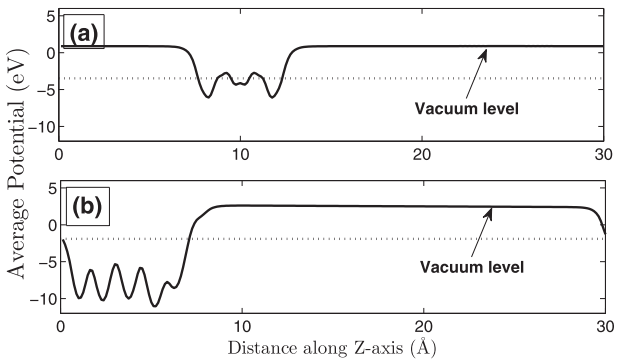

FIG. 9. The potential averaged over X-Y plane is plotted along the Z-axis: (a) for relaxed (3,3) CNT and (b) relaxed Si(001) surface with pattern-A. The vacuum levels are indicated. The dotted line in each panel indicates the fermi energy level.

substrate induced by the adsorbate.[40] Considering the fact that C is more electronegative than Si, the charge transfer from Si to C is reasonable.

Thus, we may conclude that the (3,3) CNT integrated on the Si(001) having pattern-A becomes semiconducting due to the formation of strong Si-C bonds. The Si-C bonds are partially ionic and partially covalent in nature. Also in the process of CNT adsorption, electronic charge transfers from Si surface to CNT.

As tailoring electrical properties with external means is technologically important, we now discuss the effect of an external electric field (E_{ext}) on the electrical properties of the (3,3) CNT supported on the Si(001) having pattern-A. We have completely relaxed the system for five different field strengths, namely, $E_{ext} = 0.1\,\mathrm{V/Å}$, $0.2\,\mathrm{V/Å}$, $0.3\,\mathrm{V/Å}$, $0.4\,\mathrm{V/Å}$, and $0.5\,\mathrm{V/Å}$, respectively. The electric field is directed along the negative Z-axis. Structural changes in the system due to the electric field were not visible. However, we found that the band gap around the fermi level decreases with increasing electric field strength. The variation of bandgap as a function of field strength is plotted in Fig. 10. The curve in Fig. 10 clearly indicates that the CNT on the surface undergoes a metallic transition around field strength of $0.3\,\mathrm{V/Å}$. To have a better picture, the band structure and density of states of the (3,3) CNT supported on the Si(001) having pattern-A are plotted in Fig. 11 for a field strength of $E_{ext} = 0.4\,\mathrm{V/Å}$. This figure distinctly shows metallic behavior of the CNT supported on the surface because bands are crossing the fermi level and there is finite density of states around the fermi level. We also carried out similar calculations with electric field along positive Z-direction; however, the results were found to be independent of the direction of the field.

The partial charge density of a band crossing the fermi level (see Fig. 12) shows that the charges on CNT are responsible for the metallic behavior in the presence of external electric field. Therefore, one may conclude that the electric field helps delocalizing charges for conduction. Next, we consider the (3,3) CNT supported on the Si(001) having pattern-B.

B. (3,3) CNT on Si(001) with pattern-B

Fully relaxed and energetically favorable atomic structure of (3,3) CNT on Si(001) with pattern-B is shown in Fig. 13. The binding energy of the absorbed (3,3) CNT per unit length is 0.46 eV/Å. The CNT resides 1.4 Å above the Si surface. Here, we observe that the relaxed structure prefers the *zigzag* orientation. In the process of adsorption of the CNT, four C atoms form bonds with surface Si atoms within the 4×2 supercell without breaking any C-C bonds. The C-C bond lengths are altered by a small amount. The C-C bond length varies from 1.41 to 1.5 Å with an average of 1.445 Å while the C-Si bond lengths are ≈1.99 Å. These results are very similar to that of the most favorable structure when (3,3) CNT is supported on bare Si(001): 2×1 surface.[11] In spite of strong interaction of the CNT with the surface, the hollowness of the CNT is retained with 9.7% deformation ratio. Also note from Fig. 13 that the buckling of Si dimers is destroyed and the dimers become symmetric and horizontal due to CNT adsorption. The Bader analysis shows that 2.21 e is transferred to CNT from Si surface within the 4×2 supercell. The charge density difference along a Si-C bond (not plotted here) shows similar behavior as shown in the Fig. 8 which is also an indication of charge transfer from surface to CNT. Our calculated work-function of the Si(001) having pattern-B is 4.8 eV while that for CNT is known to be 4.35 eV. Thus, in this case also the charge

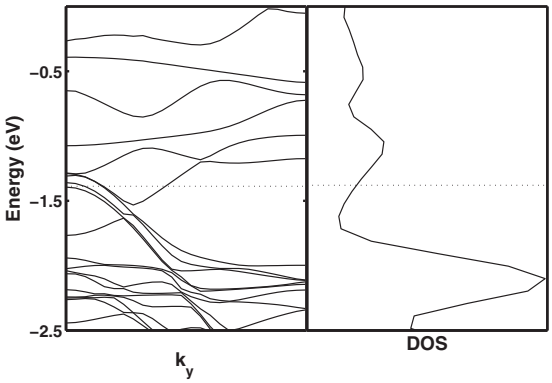

FIG. 11. The band structure and density of states for (3,3) CNT supported on the Si(001) having pattern-A in the presence of an electric field of 0.4 V/Å along -Z direction.

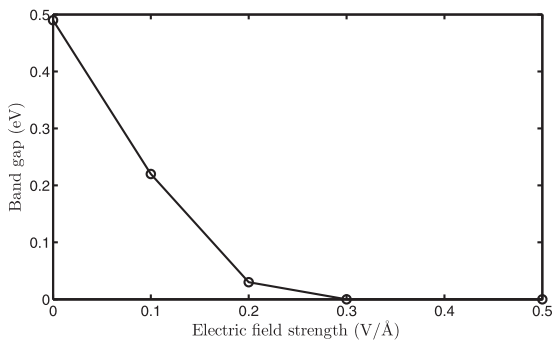

FIG. 10. The band gap of (3,3) CNT supported on Si(001) having pattern-A is plotted as a function of electric field strength. The band gap vanishes around the field strength of 0.3 V/Å.

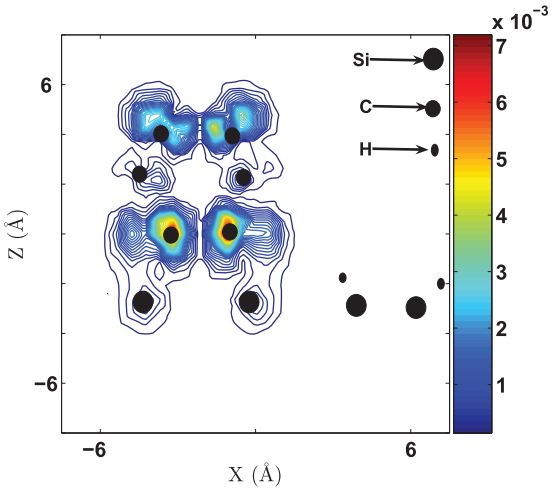

FIG. 12. The partial density corresponding to a band crossing the fermi level of the CNT supported on Si(001) having pattern-A. An external electric field of 0.4 V/Å is applied.

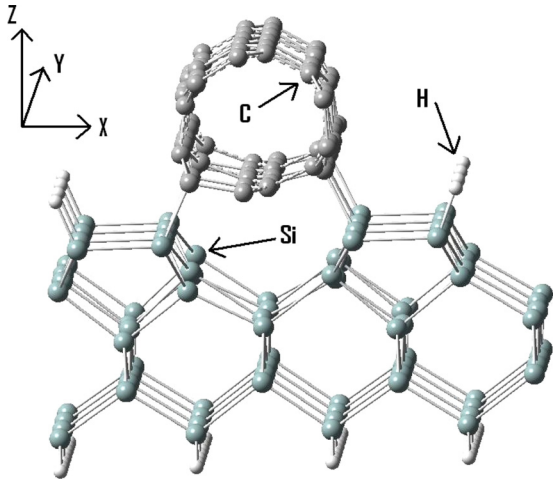

FIG. 13. The most favorable atomic structure of the CNT(3,3) placed on the hydrogen terminated Si(001) surface having pattern-B.

transfer takes place from higher to a lower work-function material.

For finding out the electrical nature, we carried out band structure analysis of the (3,3) CNT supported on the Si(001) having pattern-B. The band structure and the density of states for this system are plotted in Fig. 14, where the fermi level is represented by the dotted line. The gap of ≈0.6 eV around the fermi level is reflected in both the band structure and the density of states.

In this system, the band gap can also be tuned by applying an external electric field. We have considered an electric field directed along the negative Z-axis with various strengths from $E_{ext} = 0.01$ V/Å to $E_{ext} = 0.5$ V/Å with an increment of 0.1 V/Å. We found that the band gap reduces with the increase of the electric field strength. The gap nearly vanishes around $E_{ext} = 0.4$ V/Å which is larger compared to the case of (3,3) CNT supported on the Si(001) having pattern-A. The band structure and the density of states for the system in the presence of $E_{ext} = 0.4$ V/Å are plotted in Fig. 15, the dotted line represents the fermi level. We observe in Fig. 15 that the gap around the fermi level vanishes, band just crosses fermi level and finite density of states appears around that region. These indicate that the (3,3) CNT supported on the Si(001) having pattern-B undergoes a metallic transition induced by external electric field.

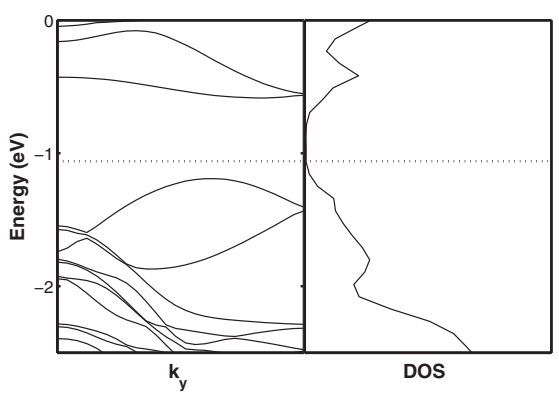

FIG. 14. The band structure and density of states of CNT(3,3) integrated on Si(001) with pattern-B. The dashed line indicates the fermi energy level.

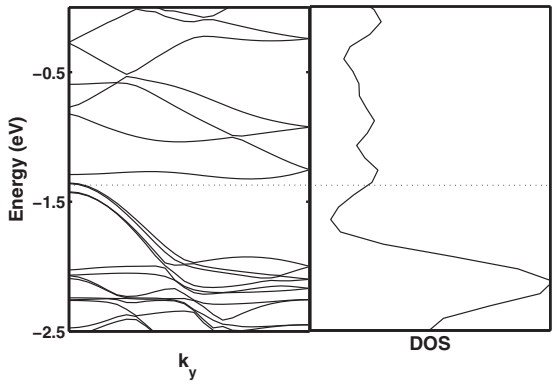

FIG. 15. The band structure and density of states for (3,3) CNT supported on the Si(001) having pattern-B in the presence of an electric field of 0.4 V/Å along -Z direction.

Comparing the results of CNT integration on both the patterned Si(001) surfaces, we find that the (3,3) CNT supported on the Si(001) having pattern-A is superior from technological point of view because it is energetically more favorable, easily distinguishable due its larger height on the surface and the bandgap may be tuned from 0.5 eV to 0.0 eV with lesser field strength.

IV. SUMMARY

We have studied the structure, energetics, and electrical properties of a (3,3) metallic CNT adsorbed on Si(001) surface having pattern-A (See Fig. 2) and pattern-B (see Fig. 3). We find that the binding energy of the CNT per unit length is 0.75 eV on the Si(001) having pattern-A and 0.46 eV on the Si(001) having pattern-B. The Si-C bond lengths are shorter and the deformation ratio of the CNT is larger in the earlier case even though total number of Si-C bonds and average C-C bond lengths are same in both the cases. Thus, (3,3) CNT is energetically more favorable on the Si(001) having pattern-A. The height of the CNT on Si(001) having pattern-A is larger by ≈0.4 Å and therefore, the CNT on the Si(001) having pattern-A may be distinguished more easily compared to that on the Si(001) having pattern-B. The (3,3) CNT on the patterned surfaces having pattern-A and pattern-B becomes semiconducting with a band gap of ≈ 0.5 eV and 0.6 eV, respectively. However, (3,3) CNT supported on Si(001) may be turned into metallic by applying an external electric field of 0.3 V/Å to 0.4 V/Å. Based on the energetics and electrical properties of (3,3) CNT supported on Si(001), we conclude that pattern-A is preferable over pattern-B for integration of (3,3) CNT on the Si(001) substrate.

ACKNOWLEDGMENTS

This work is supported in part from the Department of Energy. This research used resources of the National Energy Research Scientific Computing Center, which is supported by the office of Science of the U.S. Department of Energy under Contract No. DE-AC02-05CH11231.

[1]S. Iijima, Nature (London) **354**, 56 (1991); T. Ichihasi, *ibid.* **363**, 603 (1993).
[2]M. M. Treacy, T. W. Ebbesen, and J. M. Gibson, Nature (London) **381**, 678 (1996).

[3]J. P. Lu, Phys. Rev. Lett **79**, 1297 (1997).
[4]E. Hernández, C. Goze, P. Bernier, and A. Rubio, Phys. Rev. Lett. **80**, 4502 (1998).
[5]R. Satio, G. Dresselhaus, and M. S. Dresselhaus, *Physical Properties of Carbon Nanotubes* (Imperial College, London, 2005).
[6]R. Satio, M. Fujita, G. Dresselhaus, and M. S. Dresselhaus, Phys. Rev. B **46**, 1804–1811 (1992).
[7]R. Satio, M. Fujita, G. Dresselhaus, and M. S. Dresselhaus, Appl. Phys. Lett. **60**, 2204–2206 (1992).
[8]R. Satio, G. Dresselhaus, and M. S. Dresselhaus, J. Appl. Phys. **73**, 494 (1993).
[9]W. Orellana, R. H. Miwa, and A. Fazzio, Phys. Rev. Lett. **91**, 166802 (2003).
[10]S. Berber and A. Oshiyama, Phys. Rev. Lett. **96**, 105505 (2006).
[11]G. W. Peng, A. C. H. Huan, L. Liu, and Y. P. Peng, Phys. Rev. B **74**, 235416 (2006).
[12]S. B. Lopez, P. M. Albrecht, N. A. Romero, and K. Hess, J. Appl. Phys. **100**, 124304 (2006).
[13]R. H. Miwa, W. Orellana, and A. Fazzio, Appl. Phys. Lett. **86**, 213111 (2005).
[14]P. M. Albrecht, S. B.Lopez, and J. W. Lyding, Nanotechnology **18**, 095204 (2007).
[15]P. M. Albrecht and J. W. Lyding, Appl. Phys. Lett. **83**, 5029 (2003).
[16]T. C. Shen, C. Wang, G. C. Abein, J. R. Tucker, J. W. Lyding, Ph. Avouris, and R. E. Walkup, Science **268**, 1590–1592 (1995).
[17]J. N. Randall, J. W. Lyding, S. Schmucker, J. R. Von Ehr, J. Ballard, R. Saini, H. Xu, and Y. Ding, J. Vac. Sci. Technol. B **27**, 2764 (2009).
[18]J. J. Boland Adv. Phys. **42**, 129 (1993).
[19]F. S. Tautz and J. A. Schaefer, J. Appl. Phys. **84**, 6636 (1998).
[20]Y. J. Chabal and K. Raghavachari, Phys. Rev. Lett. **54**, 1055 (1985).
[21]J. J. Boland, Phys. Rev. Lett. **65**, 3325 (1990).
[22]J. J. Boland, Surf. Sci. **261**, 17 (1992).
[23]Y. J. Chabal and K. Raghavachari, Phys. Rev. Lett. **53**, 282 (1984).
[24]S. Konar and B. C. Gupta, Phys. Rev. B **83**, 245412 (2011).
[25]J. Y. Lee and J. H. Cho, Appl. Phys. Lett **89**, 023124 (2006).
[26]S. B. Lopez, P. M. Albrecht, and J. W. Lydig, Phys. Rev. B **80**, 045415 (2009).
[27]P. M. Albrecht and J. W. Lyding, Nanotechnology **18**, 125302 (2007).
[28]P. M. Albrecht, S. B. Lopaz, and J. W. Lyding, Small **3**, 1402–1406 (2007).
[29]N. Wang, Z. K. Tang, G. D. Li, and J. S. Chen, Nature (London) **408**, 50 (2000).
[30]G. Kresse and J. Hafner, Phys. Rev. B **47**, R558 (1993); *ibid.* **49**, 14251 (1994).
[31]G. Kresse and J. Furtmuller, Phys. Rev. B **54**, 11169 (1996).
[32]G. Kresse and J. Furtmuller, Comput. Mater. Sci. **6**, 15 (1996).
[33]G. Kresse and J. Hafner, J. Phys.: Condens. Matter **B6**, 8245 (1994).
[34]P. Sen, S. Ciraci, I. P. Batra, C. H. Grain, and S. Sivanathan, Surf. Sci. **519**, 79 (2002).
[35]C. Hobbs, L. Kantorovich, and J. D. Gale, Surf. Sci. **591**, 45 (2005).
[36]M. W. Radny, P. V. Smith, T. C. G. Rrusch, O. Warschkow, N. A. Marks, H. F. Wilson, S. R. Schofield, N. J. Curson, D. R. McKenzie, and M. Y. Simons, Phys. Rev. B **76**, 155302 (2007).
[37]M. Ceriotti and M. Bernasconi, Phys. Rev. B **76**, 245309 (2007).
[38]R. Bader, *Atoms in Molecules: A Quantum Theory* (Oxford University Press, New York, 1990).
[39]W. Tang, E. Sanvile, and G. Henkelman, J. Phys.: Condens. Matter **21**, 084204 (2009).
[40]T. C. Leung, C. L. Kao, W. S. Su, Y. J. Feng, and C. T. Chan, Phys. Rev. B **68**, 195408 (2003).